

Spin–Orbit-Induced Anomalous pH-Dependence in ^1H NMR Spectra of Co^{III} Amine Complexes: A Diagnostic Tool for Structure Elucidation

Kaspar Hegetschweiler,^{*,†} Dirk Kuppert,[†] Jochen Huppert,[†] Michal Straka,[‡] and Martin Kaupp^{*,‡}

Contribution from the Universität des Saarlandes, Anorganische Chemie, Postfach 15 11 50, D-66041 Saarbrücken, Germany, and Institut für Anorganische Chemie, Universität Würzburg, Am Hubland, D-97074 Würzburg, Germany

Received December 12, 2003; E-mail: hegetschweiler@mx.uni-saarland.de; kaupp@mail.uni-wuerzburg.de

Abstract: The pH-dependent ^1H NMR characteristics of a series of Co^{III} -(polyamin)-aqua and Co^{III} -(polyamin)-(polyalcohol) complexes, $[\text{Co}(\text{tach})(\text{ino-}\kappa^3\text{-O}^{1,3,5})]^{3+}$ (1^{3+}), $[\text{Co}(\text{tach})(\text{ino-}\kappa^3\text{-O}^{1,2,6})]^{3+}$ (2^{3+}), $[\text{Co}(\text{tach})(\text{taci-}\kappa\text{-N}^1\text{-}\kappa^2\text{-O}^{2,6})]^{3+}$ (3^{3+}), $[\text{Co}(\text{ditame})(\text{H}_2\text{O})]^{3+}$ (4^{3+}), and $[\text{Co}(\text{tren})(\text{H}_2\text{O})_2]^{3+}$ (5^{3+}), were studied in D_2O by means of titration experiments (tach = *all-cis*-cyclohexane-1,3,5-triamine, ino = *cis*-inositol, taci = 1,3,5-triamino-1,3,5-trideoxy-*cis*-inositol, tren = tris(2-aminoethyl)amine, ditame = 2,2,6,6-tetrakis(aminomethyl)-4-aza-heptane). A characteristic shift was observed for H(–C) hydrogen atoms in the α -position of a coordinated amino group upon deprotonation of a coordinated oxygen donor. For a *cis*-H–C–N–Co–O–H arrangement, deprotonation of the oxygen donor resulted in an additional shielding (shift to lower frequency) of the H(–C) proton, whereas for a *trans*-H–C–N–Co–O–H arrangement, deprotonation resulted in a deshielding (shift to higher frequency). The effect appears to be of rather general nature: it is observed for primary (1^{3+} – 5^{3+}), secondary (4^{3+}), and tertiary (5^{3+}) amino groups, and for the deprotonation of an alcohol (1^{3+} – 3^{3+}) or a water (4^{3+} , 5^{3+}) ligand. Spin–orbit-corrected density functional calculations show that the high-frequency deprotonation shift for the *trans*-position is largely caused by a differential cobalt-centered spin–orbit effect on the hydrogen nuclear shielding. This effect is conformation dependent due to a Karplus-type behavior of the spin–orbit-induced Fermi-contact shift and thus only significant for an approximately antiperiplanar H–C–N–Co arrangement. The differential spin–orbit contribution to the deprotonation shift in the *trans*-position arises from the much larger spin–orbit shift for the protonated than for the deprotonated state. This is in turn due to a *trans*-effect of the deprotonated (hydroxo or alkoxo) ligand, which weakens the *trans* Co–N bond and thereby interrupts the Fermi-contact mechanism for transfer of the spin–orbit-induced spin polarization to the hydrogen nucleus in question. The unexpectedly large long-range spin–orbit effects found here for 3d metal complexes are traced back to small energy denominators in the perturbation theoretical expressions of the spin–orbit shifts.

1. Introduction

Co^{III} -amine-aqua complexes may be regarded as one of the archetypes of an inert metal complex; they have been at the forefront of coordination chemistry for more than 130 years. The simple ammine-aqua derivatives of composition $[\text{Co}(\text{NH}_3)_x(\text{H}_2\text{O})_{6-x}]^{3+}$ ($3 \leq x \leq 5$) were extensively investigated by Jørgensen and Werner.^{1,2} These early studies established the well-known reactivity of such species, a very inert Co–N bond, a somewhat more labile (but still inert) Co–O bond, and the moderate acidity of the coordinated water molecules, which can readily be deprotonated in aqueous solution above pH 4–6.³ Corresponding complexes with chelating polyamines have been the subject of numerous subsequent studies,⁴ serving for example

as model compounds for the investigation of the kinetics and mechanism of ligand exchange reactions.⁵ Co^{III} -amine complexes with polyalcohols have been prepared as models for the elucidation of metal binding to carbohydrates.⁶ The diamagnetic Co^{III} center is particularly suitable for this purpose, because the different species formed in solution can readily be identified by conventional NMR methods.⁷

In view of the reactivity in aqueous solution, deprotonation of an aqua ligand or a coordinated hydroxy group is a

[†] Universität des Saarlandes.

[‡] Universität Würzburg.

(1) Jørgensen, S. M. Z. *Anorg. Chem.* **1898**, *17*, 455 and references therein.

(2) Werner, A. *Ber.* **1906**, *39*, 2673.

(3) Werner, A. *Ber.* **1907**, *40*, 4098.

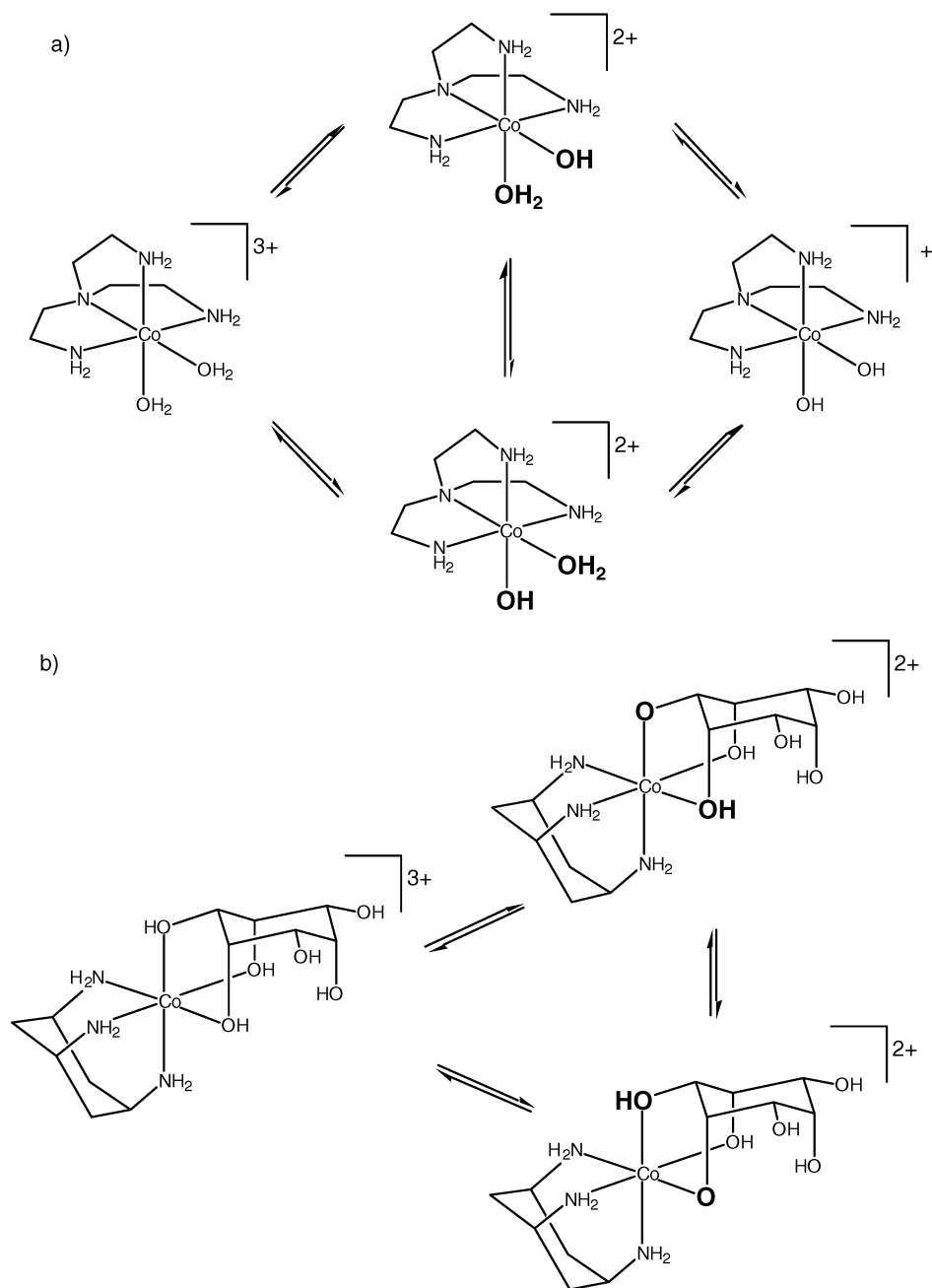
(4) House, D. A. *Compr. Coord. Chem.* **1987**, *2*, 23.

(5) (a) House, D. A. *Coord. Chem. Rev.* **1977**, *23*, 223. (b) Tobe, M. L. *Compr. Coord. Chem.* **1987**, *1*, 281.

(6) (a) Burger, J.; Klüfers, P. *Chem. Ber.* **1995**, *128*, 75. (b) Yano, S. *Coord. Chem. Rev.* **1988**, *92*, 113. (c) Tanase, T.; Onaka, T.; Nakagoshi, M.; Kinoshita, I.; Shibata, K.; Doe, M.; Fujii, J.; Yano, S. *Inorg. Chem.* **1999**, *38*, 3150. (d) Bunel, S.; Ibarra, C.; Moraga, E.; Blaskó, A.; Bunton, C. A. *Carbohydr. Res.* **1993**, *244*, 1. (e) Yamanari, K.; Nakamichi, M.; Shimura, Y. *Inorg. Chem.* **1989**, *28*, 248. (f) Harrowfield, J. M.; Mocerino, M.; Skelton, B. W.; Wei, W.; White, A. H. *J. Chem. Soc., Dalton Trans.* **1995**, 783.

(7) Hausherr-Primo, L.; Hegetschweiler, K.; Rüegger, H.; Odier, L.; Hancock, R. D.; Schmalte, H. W.; Gramlich, V. J. *Chem. Soc., Dalton Trans.* **1994**, 1689.

Scheme 1



particularly important reaction, because it has a pronounced influence on the stability and reactivity of the individual components. As an example, it has been shown that a variety of *cis*-diaqua-tetraamine-Co^{III} complexes exhibited rather high activity as catalysts for phosphate ester hydrolysis,⁸ and the active species have been identified as singly deprotonated monohydroxo derivatives such as [Co(tren)(H₂O)(OH)]²⁺ (Scheme 1a).⁹ It is noteworthy that the two water ligands in this complex are not equivalent, and, consequently, two tautomeric forms must be taken into account. In most of the deprotonation studies

reported in the literature, only the macroscopic $\text{p}K_{\text{a}}$ values have been determined. It has, however, been shown that solvent molecules bonded to the two sites *p* and *t* (i.e., trans to the primary or to the tertiary nitrogen donor) showed a distinctly different reactivity.¹⁰ To develop a better understanding of the mechanisms of such reactions, it would be of value to know the individual acidities of the two water ligands H₂O^{*p*} and H₂O^{*t*}. An analogous situation arises when the water ligands are replaced by a chelating polyalcohol (Scheme 1b). As in the case of the aqua derivatives, the individual acidity of the different types of coordinated hydroxy groups has a significant influence on the pH-dependent species distribution in aqueous solutions.⁷ The analysis of such a microscopic deprotonation scheme has, however, proven to be rather difficult. For [Co(tren)(H₂O)₂]³⁺,

(8) (a) Norman, P. R.; Cornelius, R. D. *J. Am. Chem. Soc.* **1982**, *104*, 2356. (b) Jones, D. R.; Lindoy, L. F.; Sargeson, A. M. *J. Am. Chem. Soc.* **1983**, *105*, 7327. (c) Rawji, G.; Hediger, M.; Milburn, R. M. *Inorg. Chim. Acta* **1983**, *79*, 247. (d) Kenley, R. A.; Fleming, R. H.; Laine, R. M.; Tse, D. S.; Winterle, J. S. *Inorg. Chem.* **1984**, *23*, 1870.
(9) (a) Chin, J.; Zou, X. *J. Am. Chem. Soc.* **1988**, *110*, 223. (b) Chin, J.; Banaszczuk, M.; Jubian, V.; Zou, X. *J. Am. Chem. Soc.* **1989**, *111*, 186.

(10) Curtis, N. J.; Lawrance, G. A. *J. Chem. Soc., Dalton Trans.* **1985**, 1923.

Buckingham and co-workers performed a detailed ^{17}O NMR study and estimated the equilibrium constant K_T for the two tautomeric mono-hydroxo forms as $K_T = 3.2$, with a preference of the first deprotonation at the H_2O^p water ligand.¹¹ However, ^{17}O NMR spectroscopy still does not represent a routine technique. Moreover, this method is only applicable to a limited number of aqua complexes and is not suited for the polyalcohol derivatives, unless the ambitious task of preparing correspondingly ^{17}O -labeled polyalcohol ligands is pursued.

The pH-dependence of ^1H resonances in organic acids and bases has frequently been used to determine the microscopic dissociation constant of a specific functional group.^{12,13} Protonation of a basic site usually results in a deshielding of the nearby H(-C) protons, and this can readily be detected by routine ^1H NMR titration experiments (δ versus pH plots). The deshielding effect increases with decreasing distance and is often discussed in oversimplified terms of a withdrawal of electron density. For organic polyamines, an effective correlation using a set of empirically deduced deshielding parameters has been derived to estimate the deshielding of the different C-H protons.

One might expect that the deprotonation of a coordinated OH group of an aqua or alcohol ligand would, by analogy, increase the electron density on the metal center and subsequently within the organic ligand framework. Following the crude notion of a correlation between charge and chemical shift, corresponding low-frequency shifts in the ^1H NMR spectrum should be observable. In our ongoing investigation on the coordination chemistry of polyalcohol- and polyamino-polyalcohol ligands,¹⁴ we have indeed observed a characteristic dependence of the various ^1H resonances on pH. For the resonances belonging to the (C-H) protons which are in α -position to the deprotonated oxygen donor, the observed shift always behaved as expected. However, when examining hydrogen atoms in α -position to a coordinated amino group, some of the signals displayed the opposite behavior. This effect, which appears to have escaped previous systematic observations, has considerable potential for a straightforward elucidation of an individual deprotonation scheme. We wish to report the relevant NMR characteristics and show theoretically, by appropriate density functional methods, that this hitherto unrecognized effect is due to unusually large long-range spin-orbit effects originating at the cobalt metal center.

2. Experimental Section

Materials. The Co^{III} complexes¹⁵ $[\text{Co}(\text{tach})(\text{H}_{-1}\text{ino}-\kappa^3\text{-O}^{1,3,5})](\text{NO}_3)_2$,⁷ $[\text{Co}(\text{tach})(\text{taci}-\kappa\text{-N}^1-\kappa^2\text{-O}^{2,6})](\text{NO}_3)_3 \cdot 3\text{H}_2\text{O}$,¹⁶ $[\text{Co}(\text{ditame})(\text{H}_2\text{O})](\text{CF}_3\text{SO}_3)_3$,¹⁷ and $[\text{Co}(\text{tren})(\text{H}_2\text{O})_2](\text{CF}_3\text{SO}_3)_3$ ¹⁸ were prepared as described in the literature.

- (11) Brasch, N. E.; Buckingham, D. A.; Clark, C. R.; Rogers, A. J. *Inorg. Chem.* **1998**, *37*, 4865.
- (12) (a) Sudmeier, J. L.; Reilley, C. N. *Anal. Chem.* **1964**, *36*, 1698. (b) Blaskó, A.; Bunton, C. A.; Bunel, S.; Ibarra, C.; Moraga, E. *Carbohydr. Res.* **1997**, *298*, 163–172.
- (13) (a) Delgado, R.; Frausto Da Silva, J. J. R.; Amorim, M. T. S.; Cabral, M. F.; Chaves, S.; Costa, J. *Anal. Chim. Acta* **1991**, *245*, 271. (b) Lumry, R.; Smith, E. L.; Glantz, R. R. *J. Am. Chem. Soc.* **1951**, *73*, 4330.
- (14) Hegetschweiler, K. *Chem. Soc. Rev.* **1999**, *28*, 239.
- (15) Abbreviation of ligands: tach = all-cis-cyclohexane-1,3,5-triamine, ino = cis-inositol, taci = 1,3,5-triamino-1,3,5-trideoxy-cis-inositol, tren = tris-(2-aminoethyl)amine, ditame = 2,2,6,6-tetrakis(aminomethyl)-4-aza-heptane.
- (16) Ghisletta, M.; Hausherr-Primo, L.; Gajda-Schranz, K.; Machula, G.; Nagy L.; Schmalle, H. W.; Rihs, G.; Endres, F.; Hegetschweiler, K. *Inorg. Chem.* **1998**, *37*, 997.

NMR Measurements. ^1H and $^{13}\text{C}\{^1\text{H}\}$ NMR spectra were measured in D_2O (28 °C) using a Bruker DRX 500 spectrometer (resonance frequencies: 500.13 MHz for ^1H and 125.9 MHz for ^{13}C). Chemical shifts (in ppm) are given relative to sodium (trimethylsilyl)propionate- d_4 as an internal standard (=0 ppm). The pH of each sample was adjusted using appropriate solutions of DCl and NaOD in D_2O . A Hamilton SPINTRODE glass electrode, fitted with an internal Ag/AgCl reference (H_2O), which was calibrated with aqueous (H_2O) buffer solutions, was used within the NMR tube for the measurement of pH^* (the direct pH-meter reading, $\text{pD} = -\log[\text{D}^+]$ was calculated as $\text{pD} = \text{pH}^* + 0.4$).¹³ The pH^* was checked prior to and after each measurement. The buffering capacity of the Co complexes was sufficient, and no additional buffer was required. Least squares calculations ($\sum(\delta_{\text{obs}} - \delta_{\text{calc}})^2 = \text{min}$) were performed using the computer program NMR-Tit;¹⁹ the resulting parameters (pK_a and δ_{calc}) of the macro species are collected in Table S1. Two-dimensional NMR experiments were performed according to the literature.²⁰

3. Details of Quantum Chemical Calculations

In addition to the experimentally studied system $[\text{Co}(\text{H}_2\text{O})-(\text{ditame})]^{3+}/[\text{Co}(\text{OH})(\text{ditame})]^{2+}$ ($4^{3+}/4\text{-H}^{2+}$), most calculations focused on simplified model systems, to enable more detailed analyses. Model $6^{3+}/6\text{-H}^{2+}$ consisted of the $[\text{Co}(\text{en})(\text{H}_2\text{O})-(\text{NH}_3)_3]^{3+}$ complex and the corresponding aqua ligand deprotonation product (see Figure 3). The still simpler model $7^{3+}/7\text{-H}^{2+}$, which was used to study the conformational dependence of chemical shifts, started from the *trans*- $[\text{Co}(\text{NH}_3)_4(\text{NH}_2\text{Me})(\text{H}_2\text{O})]^{3+}$ complex and deprotonated again the aqua ligand (cf. Figure 5). The structures of all of the complexes were fully optimized (cf. Table S2 in Supporting Information) at the density functional theory (DFT) level, using the B3LYP hybrid functional,²¹ TZVP basis sets,²² and the Turbomole 5.6 program.²³

DFT calculations of nuclear shielding tensors used the deMon-KS²⁴ and deMon-NMR²⁵ programs and applied the gradient-corrected BP86 functional.²⁶ A 9s7p4d basis set²⁷ was used for cobalt, together with a modified Huzinaga-type

- (17) Hegetschweiler, K.; Maas, O.; Zimmer, A.; Geue, R. J.; Sargeson, A. M.; Harmer, J.; Schweiger, A.; Buder, I.; Schwitzgebel, G.; Reiland, V.; Frank, W. *Eur. J. Inorg. Chem.* **2003**, 1340.
- (18) Düpre, Y.; Bartscherer, E.; Maas, O.; Sander, J.; Hegetschweiler, K. Z. *Kristallogr. New Cryst. Struct.* **1999**, *214*, 407.
- (19) Ries, A.; Hegetschweiler, K. *NMR-Tit, Program for the Simulation of pH Dependent Shifts in NMR Spectra*, Version 2.0; Saarbrücken, 1999.
- (20) (a) Hurd, R. E. *J. Magn. Reson.* **1990**, *87*, 422. (b) von Kienlin, M.; Moonen, C. T. W.; van der Toorn, A.; van Zijl, P. C. M. *J. Magn. Reson.* **1991**, *93*, 423. (c) Hurd, R. E.; John, B. K. *J. Magn. Reson.* **1991**, *91*, 648. (d) Ruiz-Cabello, J.; Vuister, G. W.; Moonen, C. T. W.; van Gelderen, P.; Cohen, J. S.; van Zijl, P. C. M. *J. Magn. Reson.* **1992**, *100*, 282. (e) Wilker, W.; Leibfritz, D.; Kerssebaum, R.; Bermel, W. *Magn. Reson. Chem.* **1993**, *31*, 287.
- (21) Becke, A. D. *J. Chem. Phys.* **1993**, *98*, 5648. Lee, C.; Yang, W.; Parr, G. R. *Phys. Rev. B* **1988**, *37*, 785. Miehlich, B.; Savin, A.; Stoll, H.; Preuss, H. *Chem. Phys. Lett.* **1989**, *157*, 200.
- (22) Schäfer, A.; Huber, C.; Ahlrichs, R. *J. Chem. Phys.* **1994**, *100*, 5829.
- (23) Ahlrichs, R.; Bär, M.; Häser, M.; Horn, H.; Kölmel, C. *Chem. Phys. Lett.* **1989**, *162*, 165. See also: Ahlrichs, R.; von Arnim, M. In *Methods and Techniques in Computational Chemistry: METECC-95*; Clementi, E., Corongiu, G., Eds.; Club Européen MOTECC, 1995; Chapter 13, p 509ff.
- (24) (a) Salahub, D. R.; Fournier, R.; Mlynarski, P.; Papai, I.; St-Amant, A.; Ushio, J. In *Density Functional Methods in Chemistry*; Labanowski, J., Andzelm, J., Eds.; Springer: New York, 1991. (b) St-Amant, A.; Salahub, D. R. *Chem. Phys. Lett.* **1990**, *169*, 387.
- (25) Malkin, V. G.; Malkina, O. L.; Eriksson, L. A.; Salahub, D. R. In *Modern Density Functional Theory: A Tool for Chemistry; Theoretical and Computational Chemistry*; Seminario, J. M., Politzer, P., Eds.; Elsevier: Amsterdam, 1995; Vol. 2.
- (26) Becke, A. D. *Phys. Rev. A* **1988**, *38*, 3098. Perdew, J. P.; Wang, Y. *Phys. Rev. B* **1986**, *33*, 8822.
- (27) Munzarová, M.; Kaupp, M. *J. Phys. Chem. A* **1999**, *103*, 9966. This basis set is derived from the basis by: Schäfer, A.; Horn, H.; Ahlrichs, R. *J. Chem. Phys.* **1992**, *97*, 2571.

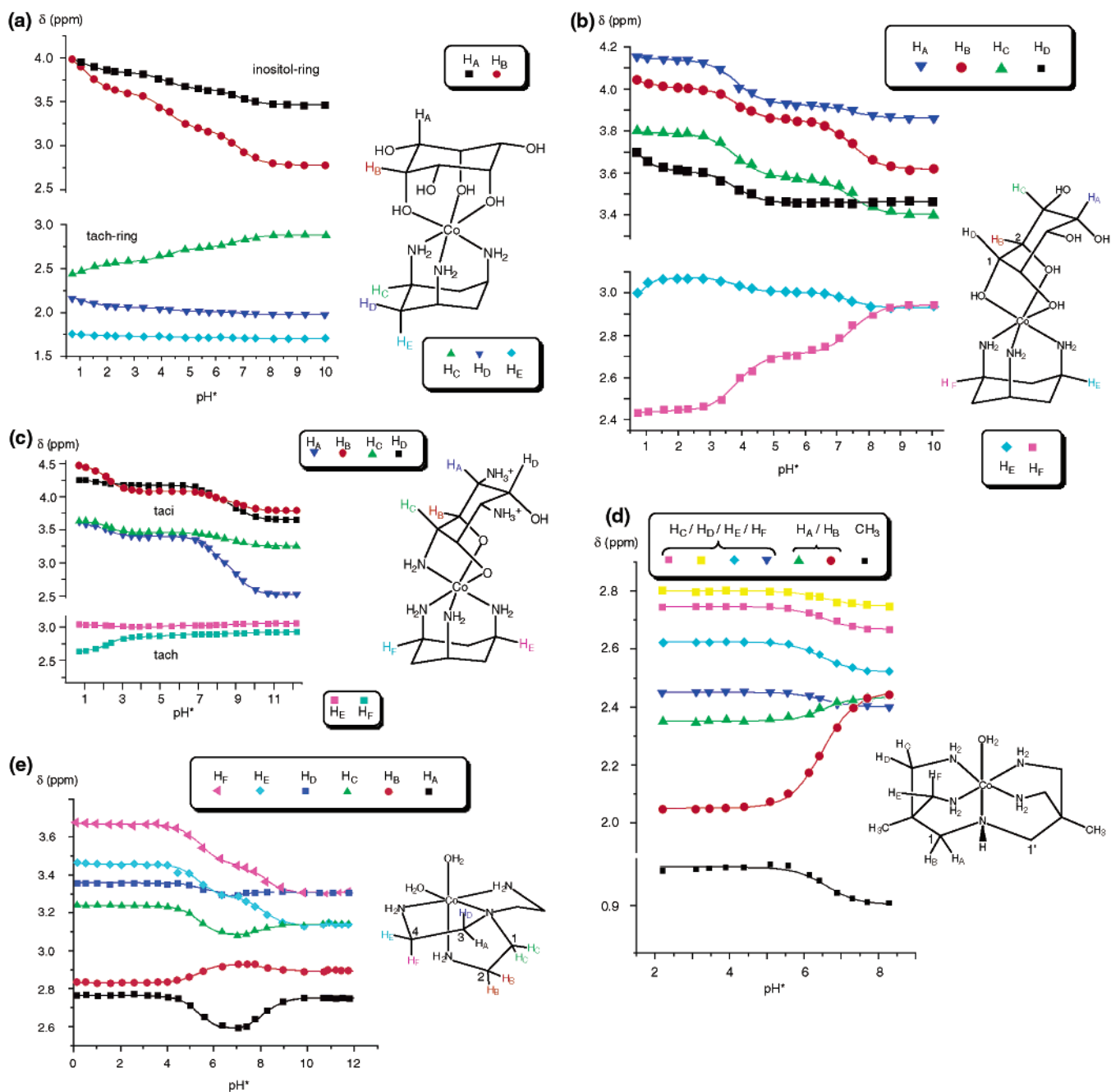


Figure 1. pH-dependence of the ^1H NMR resonances of (a) $[\text{Co}(\text{tach})(\text{ino-}\kappa^3\text{-O}^{1,3,5})]^{3+}$ (1^{3+}), (b) $[\text{Co}(\text{tach})(\text{ino-}\kappa^2\text{-O}^{2,4}\text{-}\kappa\text{-N}^3)]^{3+}$ (2^{3+}), (c) $[\text{Co}(\text{tach})(\text{taci-}\kappa\text{-N}^1\text{-}\kappa^2\text{-O}^{2,6})]^{3+}$ (3^{3+}), (d) $[\text{Co}(\text{ditame})(\text{H}_2\text{O})]^{3+}$ (4^{3+}), and (e) $[\text{Co}(\text{tren})(\text{H}_2\text{O})_2]^{3+}$ (5^{3+}) together with a representation of the molecular structure and the labeling scheme. The points correspond to the experimental values, and the lines are calculated (minimization of $[\delta_{\text{obs}} - \delta_{\text{calc}}]^2$) assuming a rapid equilibrium between the variably protonated species. pH^* indicates the pH-meter reading for a glass electrode (H_2O), which was calibrated with aqueous (H_2O) buffer solutions. The true pD ($= -\log[\text{D}^+]$) may be calculated as $\text{pD} = \text{pH}^* + 0.4$.¹³

basis set (termed IGLO-II)²⁸ for the ligand atoms. The initial nonrelativistic calculations were done at the SOS-DFPT level in its Loc1 approximation,^{25,29} using individual gauges for localized orbitals (IGLO²⁸). Subsequent calculations of spin-orbit (SO) corrections to the nuclear shieldings used the combined finite-perturbation/SOS-DFPT triple-perturbation method of ref 30, with a common gauge origin at the cobalt atom and a finite Fermi-contact perturbation of $\lambda = 0.001$ au

at the hydrogen atom under investigation. The Breit–Pauli one- and two-electron SO operators were described within the accurate and efficient atomic meanfield approximation,³¹ as implemented in the AMFI program.³²

Absolute nuclear shieldings were converted to relative chemical shifts using the computed shielding value of 31.02

(28) Kutzelnigg, W.; Fleischer, U.; Schindler, M. *NMR—Basic Principles and Progress*; Springer: Heidelberg, 1990; Vol. 23, p 165ff.

(29) Malkin, V. G.; Malkina, O. L.; Casida, M. E.; Salahub, D. R. *J. Am. Chem. Soc.* **1994**, *116*, 5898.

(30) (a) Malkina, O. L.; Schimmelpfennig, B.; Kaupp, M.; Hess, B. A.; Chandra, P.; Wahlgren, U.; Malkin, V. G. *Chem. Phys. Lett.* **1998**, *296*, 93. (b) Vaara, J.; Malkina, O. L.; Stoll, H.; Malkin, V. G.; Kaupp, M. *J. Chem. Phys.* **2001**, *114*, 61.

(31) Hess, B. A.; Marian, C. M.; Wahlgren, U.; Gropen, O. *Chem. Phys. Lett.* **1996**, *251*, 365.

(32) The AMFI code used is due to: Schimmelpfennig, B. *Atomic Spin-Orbit Mean-Field Integral Program*; Stockholms Universitet: Sweden, 1996.

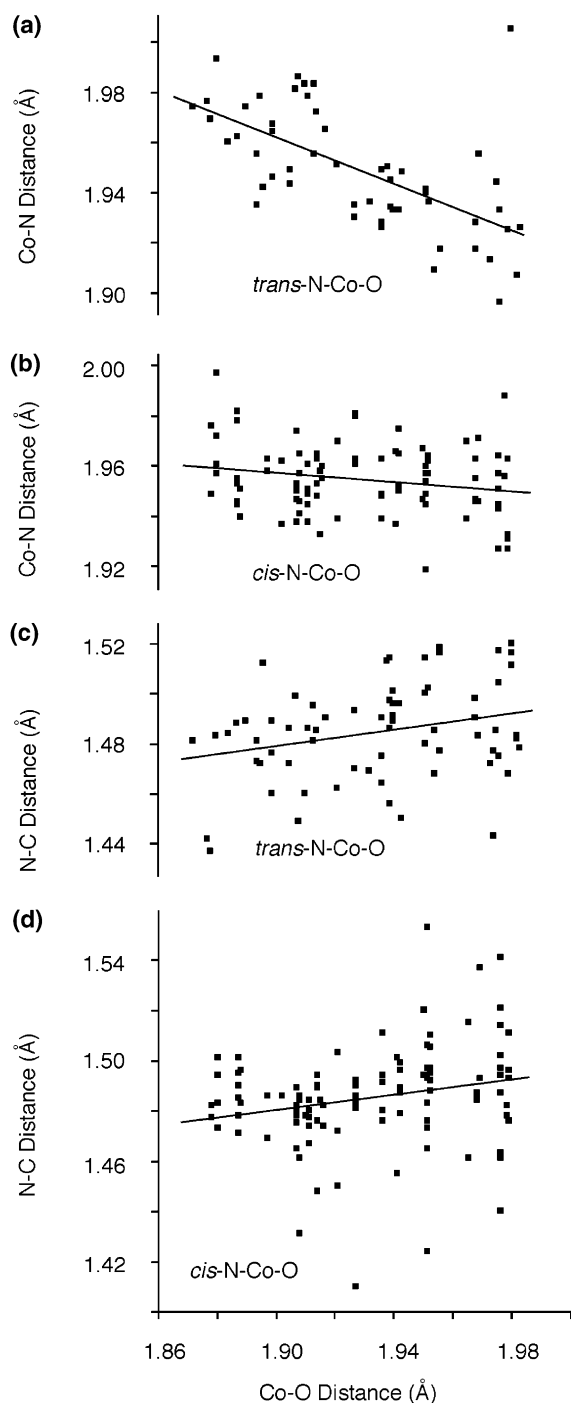


Figure 2. Dependence of the Co–N and N–C bond distances on the Co–O bond lengths in Co^{III} complexes in the $\text{H}-\text{CR}_2-\text{NR}_2-\text{Co}-\text{O}$ fragment ($\text{R} = \text{H}$, alkyl) and a *cis*- or *trans*-N–Co–O geometry as indicated. O refers to a H_2O , OH^- , ROH , or RO^- ligand. The data were obtained from the CSD database ($R < 8\%$).

ppm for $\text{Si}(\text{CH}_3)_4$ (TMS) as reference (computed with Si–C and Si–H distances of 1.875 and 1.1055 Å, respectively, and an Si–C–H angle of 111.3°). The SO ^1H shielding obtained for TMS is small (< 0.01 ppm) and was neglected. In addition to the data presented throughout the paper, various test calculations on models $6^{3+}/6\text{-H}^{2+}$ and $7^{3+}/7\text{-H}^{2+}$ were done, using larger basis sets, different gauges, and different density functionals. Despite minor quantitative differences, the qualitative conclusions of this work are not affected by these variations.

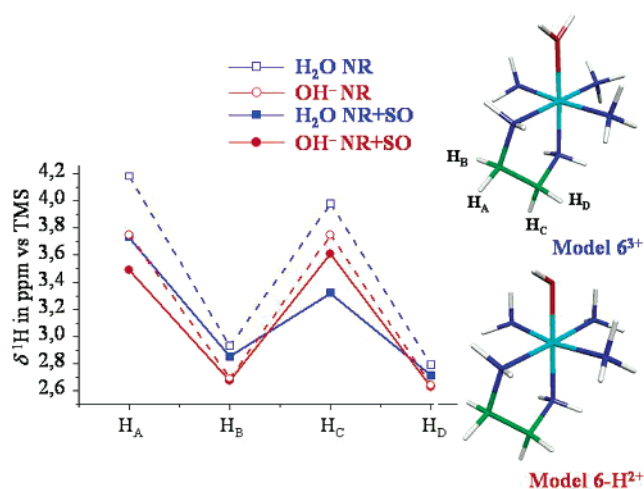


Figure 3. Computed ^1H chemical shifts for the model complexes $6\text{-H}^{2+}/6^{3+}$. Nonrelativistic results (open symbols) and results after addition of SO corrections (solid symbols). Labels for hydrogen positions are provided in the model on the right side.

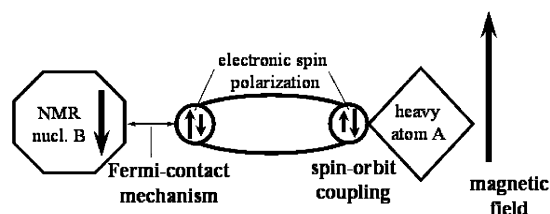


Figure 4. Schematic representation of the Fermi-contact mechanism of spin–orbit chemical shifts (cf. ref 42).

4. Results and Discussion

4.1. Experimental Results. The pH-dependent chemical shifts in the ^1H NMR spectra of the Co^{III} complexes $[\text{Co}(\text{tach})(\text{ino}-\kappa^3-\text{O}^{1,3,5})]^{3+}$ (1^{3+}), $[\text{Co}(\text{tach})(\text{ino}-\kappa^2-\text{O}^{2,4}-\kappa-\text{N}^3)]^{3+}$ (2^{3+}), $[\text{Co}(\text{tach})(\text{taci}-\kappa-\text{N}^{1-\kappa^2}-\text{O}^{2,6})]^{3+}$ (3^{3+}), $[\text{Co}(\text{ditame})(\text{H}_2\text{O})]^{3+}$ (4^{3+}), and $[\text{Co}(\text{tren})(\text{H}_2\text{O})_2]^{3+}$ (5^{3+}) together with schematic representations of their molecular structures and labeling schemes are shown in Figure 1. A list of the abbreviations used for the various ligands is given in ref 15. The complexes were applied as the trifluoromethanesulfonate or the nitrate salts. Crystal structures of the complexes 1-H^{2+} , 3^{3+} , and 5^{3+} have been reported.^{7,16,17} For the $\text{Co}(\text{ditame})^{3+}$ moiety, the crystal structures of the corresponding ammine, chloro, peroxo, and superoxo complexes are known.^{17,33} The asymmetric inositol complex 2^{3+} and its deprotonation products were observed as minor species in equilibrated solutions of 1^{3+} .⁷ For all five complexes, a series of ^1H NMR spectra was recorded as a function of pH, and the pH-dependence of the resonances was modeled assuming a rapid equilibrium between the different deprotonation products with averaged shifts for the individual protons (Figure 1). Corresponding values for the calculated shifts and the evaluated pK_a values of the various species are provided as Supporting Information (Table S1).

The pH-dependent ^1H NMR characteristics (Figure 1a) of the inositol moiety in the C_{3v} -symmetric complex 1^{3+} have been previously described.⁷ As expected, increasing deprotonation of the coordinated hydroxy groups resulted in increased shielding (shift to lower frequencies) of the two resonances H_A and

(33) Fabius, B.; Geue, R. J.; Hazell, R. G.; Jackson, W. G.; Larsen, F. K.; Qin, C. J.; Sargeson, A. M. *J. Chem. Soc., Dalton Trans.* **1999**, 3961.

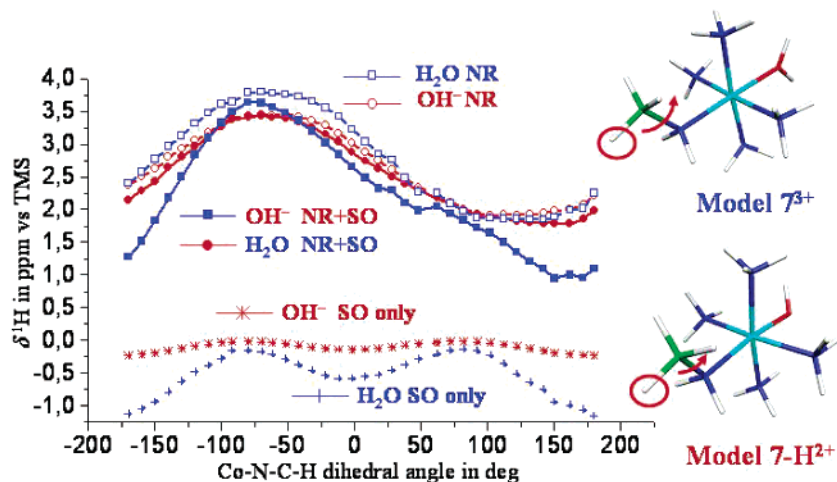


Figure 5. Computed ^1H chemical shifts for the CH_3 proton in model complexes $7\text{-H}^{2+}/7^{3+}$ (cf. left part of figure) as a function of the $\text{H}-\text{C}-\text{N}-\text{Co}$ dihedral angles. Nonrelativistic results (open squares and circles) and results after addition of SO corrections (solid squares and circles) are provided, together with the SO contributions to the shifts alone (crosses). Molecular structures are indicated on the right side of the figure.

H_B , and this effect decreased with the increasing number of bonds between the deprotonated OH group and the $(\text{C}-)\text{H}$ hydrogen under consideration. However, inspection of the pH-dependent shifts in the tach ligand revealed some unexpected behavior (Figure 1a). The three hydrogen atoms H_C , H_D , and H_E could unambiguously be assigned by $^{13}\text{C}-^1\text{H}$ and $^1\text{H}-^1\text{H}$ COSY experiments. Due to the rather large distances between these hydrogen atoms and the deprotonated hydroxy groups, one would expect rather small changes. This is indeed observed for H_D and H_E . However, deprotonation of 1^{3+} resulted in surprisingly large changes in the shift of H_C . Moreover, this change appears to go in the “wrong” direction. H_C is deshielded with increasing deprotonation.

A related behavior was observed for the C_5 -symmetric side-on isomer 2^{3+} (Figure 1b). Within the inositol ligand, all resonances again shift to lower frequency with increasing deprotonation. In the tach moiety, the largest shifts are observed for H_E and the two symmetry-equivalent H_F hydrogen atoms which are in α -position to the amino groups. Strangely enough, these two resonances showed a completely different pH-dependence. At $\text{pH} < 2$, where the abstraction of the first proton occurred, H_E is deshielded with increasing pH, whereas the chemical shift of H_F is virtually unaffected. Above pH 3, the chemical shift of H_E is moved into the other direction (to lower frequency), whereas H_F is strongly deshielded. Obviously, the first deprotonation step occurred preferentially at the equatorial hydroxy group (attached to $\text{C}1$), whereas the second and third deprotonation steps occurred at the two axial hydroxy groups attached to $\text{C}2$ and $\text{C}2'$. The only obvious difference which could account for the unexpected behavior of H_E and H_F is their geometric orientation with respect to the deprotonated oxygen donor: the resonance of the $\text{H}(\text{C})$ protons bound to the amino group with a $\text{cis-N}-\text{Co}-\text{O}$ geometry is shifted to lower frequency upon deprotonation, whereas that of the $\text{H}(\text{C})$ proton in the trans -position is shifted to higher frequency. This explanation is consistent with the behavior described above for 1^{3+} . Because of the rapid proton transfer in aqueous solution, removal of one proton must be considered as an addition of $1/3$ of a negative charge to each oxygen in the C_{3v} -symmetric cation. One trans - and two cis -effects must thus be considered for

each $(\text{N}-\text{C}-)\text{H}$ hydrogen atom, and the larger trans -effect predominates.

The taci/tach complex 3^{3+} is a further example which supported this hypothesis (Figure 1c). In this case, the two nonligated amino groups of the side-on-bonded taci ligand serve as internal bases, and, in slightly acidic solutions, the ligand is present in a zwitterionic form with two coordinated alkoxo groups and two ammonium groups. Addition of base resulted simply in the deprotonation of these ammonium groups, and this has no significant influence on the resonances of the tach moiety. However, in a more acidic medium, one of the coordinated alkoxo groups is protonated (formation of $\text{H}3^{4+}$), and it is again the hydrogen atom H_F (being in a $\text{H}-\text{C}-\text{trans-N}-\text{Co}-\text{O}$ position) which shows a reverse shift.³⁴ The hydrogen atom in the cis -position (H_E) showed no significant shift.

The ditame complex 4^{3+} is particularly suited for further examination of this effect (Figure 1d). In the C_5 -symmetric complex, a complete assignment of all ^1H resonances was not possible. However, the two hydrogens H_A and H_B bound to $\text{C}1$ could be identified due to the long-range coupling to the symmetry-equivalent $\text{C}1'$. This assignment was further supported by the observation that the corresponding double doublet of this AX-system collapsed to a singlet in 1 M NaOH (fast $\text{N}-\text{H}$ -proton exchange at the secondary nitrogen with an averaged C_{2v} structure).³⁵ Inspection of the pH-dependent shifts established that the ^1H resonances of this CH_2 group are deshielded upon deprotonation of the water ligand, and this CH_2 group is indeed attached to the nitrogen atom that is trans to the water ligand. All other CH_2 groups are bound to primary amino groups with a $\text{cis-N}-\text{Co}-\text{OH}_2$ linkage. As expected, they exhibit the “normal” slight shift to lower frequency upon deprotonation of the water ligand.

The nonequivalence of the two water ligands in the tren complex 5^{3+} has already been mentioned (Scheme 1). A series of 2D-experiments allowed a complete assignment of all resonances in the C_5 -symmetric cation. The $\text{H}_\text{B}-\text{H}_\text{C}$ portion was

(34) Based on symmetry considerations, the proton must again be assumed to be distributed equally on $\text{O}(2)$ and $\text{O}(6)$. Therefore, one trans - and one cis -effect are operative with the trans -effect being predominant.

(35) (a) Buckingham, D. A.; Clark, C. R.; Rogers, A. J. *J. Am. Chem. Soc.* **1997**, *119*, 4050. (b) Clarkson, A. J.; Buckingham, D. A.; Rogers, A. J.; Blackman, A. G.; Clark, C. R. *Inorg. Chem.* **2000**, *39*, 4769.

located as an independent AA'–XX' spin-system in a ^1H – ^1H COSY experiment. The observation of a long-range coupling to C3 allowed identification of H_C . Similarly, the H(–C3)-hydrogens were identified by their long-range coupling to C1. The differentiation between $\text{H}_\text{E}/\text{H}_\text{F}$ or $\text{H}_\text{A}/\text{H}_\text{D}$ is based on the different ^1H – ^1H coupling constants of 13 Hz (geminal), and 13, 6, 5, and 0 Hz (vicinal). These values correspond well³⁶ to the torsional H–C–C–H angles of 162°, 44°, 41°, and 77°, respectively, observed in the X-ray structure.¹⁸ The pH-dependence of the ^1H NMR signals shown in Figure 1e exhibits only two resonances with a monotonic shift toward lower frequency upon deprotonation. These two resonances correspond to H_E and H_F . It is noteworthy that these two hydrogen atoms have an exclusive cis-orientation to both water ligands. The other four hydrogen atoms all have a cis-orientation to one water molecule and a trans-orientation to the other. Interestingly, their resonances showed a nonmonotonic behavior as a function of pH. H_B exhibits a deshielding with increasing pH in the range $4 < \text{pH} < 7$, followed by some shielding in the range $7 < \text{pH} < 9$. The other three hydrogen atoms, H_A , H_C , and H_D , exhibit the reverse behavior with a shift to lower frequency in the range $4 < \text{pH} < 7$ and a shift to higher frequency in the range $7 < \text{pH} < 9$. Interestingly, this effect is rather small for H_D , and significantly larger for H_A and H_C . An unequivocal interpretation of these findings is provided by the differential acidities of the two water molecules. As mentioned above,¹¹ the $\text{H}_2\text{O}^\text{p}$ ligand is more acidic and is predominantly deprotonated in the first buffer region ($4 > \text{pH} > 7$), whereas the somewhat less acidic $\text{H}_2\text{O}^\text{i}$ is predominantly deprotonated in the second buffer region ($7 < \text{pH} < 9$). The differential acidity of the two water ligands is very nicely reflected in the corresponding plot of δ versus pH representation.

4.2. Discussion of Experimental Results. ^1H NMR characteristics of Co^III amine aqua complexes have been studied extensively,³⁷ and the mutual influence of the ligands in the cis- and trans-positions has been discussed.³⁸ The deshielding, observed in our study for a *trans*-H–C–N–Co–OH structure upon deprotonation, seems also to appear in Co^III complexes with imidazole ligands.³⁹ However, to the best of our knowledge, the markedly different shielding properties of hydrogen atoms having either a *cis*-H–C–N–Co–O or a *trans*-H–C–N–Co–O orientation upon deprotonation of the oxygen donor have not previously been recognized.

The experimental observations of this study can be summarized by the following empirical rules:

(i) In a Co^III complex with an H–C–N(R)₂–Co–O(R)–H arrangement (R = H, alkyl), deprotonation of the oxygen donor results in a characteristic shift of the H(–C) resonance in the ^1H NMR spectrum. The direction of this shift depends on the

geometry of the N–Co–O substructure. For a cis-arrangement, the resonance is shifted to lower frequency upon deprotonation, whereas for a trans-arrangement, a shift to higher frequency is observed.

(ii) As a general trend, it appears that the trans-effect is somewhat larger than the cis-effect. However, the extent of the shifts varies considerably for different hydrogen atoms even within the same molecule (see, for instance, H_A and H_D of $\mathbf{5}^{3+}$). For the complexes investigated in this study, the observed shift (for each abstracted proton) falls in the range of -0.01 to -0.12 ppm and $+0.01$ to $+0.41$ ppm for a cis- or a trans-geometry, respectively.

(iii) If several symmetry-equivalent O(R)H moieties are attached to the Co^III center in such a way that a cis- and a trans-effect operate simultaneously, the trans-effect is generally predominant (see $\mathbf{1}^{3+}$, $\mathbf{2}^{3+}$, and $\mathbf{H3}^{3+}$ as examples).

(iv) In complexes with some inequivalent O(R)H moieties, the different acidities of the individual OH groups will result in a well-defined deprotonation sequence. This is reflected in a characteristic, nonmonotonic pH-dependence of any particular resonance, where shielding and deshielding are observed for the same hydrogen atom at different pH-ranges, depending on which OH group (cis or trans) is deprotonated (see $\mathbf{5}^{3+}$).

(v) The effect is remarkably robust and independent of the chemical nature of the ligands used. It is observed for primary ($\mathbf{1}^{3+}$ – $\mathbf{5}^{3+}$), secondary ($\mathbf{4}^{3+}$), and tertiary ($\mathbf{5}^{3+}$) amino groups, and for the deprotonation of OH groups of an alcohol ($\mathbf{1}^{3+}$ – $\mathbf{3}^{3+}$) or a water ($\mathbf{4}^{3+}$, $\mathbf{5}^{3+}$) ligand.

It is often assumed that ^1H chemical shifts are primarily a function of the local electron density at the nuclei. A neutral oxygen donor of a coordinated water or alcohol ligand is generally considered a moderate σ - and a very weak π -donor. A negative oxygen donor of the corresponding hydroxo or alkoxo group is a strong σ - and a moderate (but significant) π -donor. The saturated, neutral nitrogen donor is an exclusive σ -donor. It is also well known that the deprotonation of a neutral oxygen in a Co^III -amine-aqua or Co^III -amine-alcohol complex results in a significant shortening of the Co–O bond, indicating enhanced bonding with the now negatively charged ligand (although in terms of simple ligand-field considerations, the additional p–d– π -overlap of the d^6 -low-spin configuration would enlarge antibonding interactions⁴⁰). It would thus be of interest to see whether the different behavior of the *cis*- and *trans*-H–C–N–Co–O geometry in the NMR experiments is paralleled by corresponding changes in the Co–N and C–N bond distances. A search for Co^III complexes containing saturated amines, water, hydroxide, alcohol, or alkoxo groups as ligands was performed in the Cambridge Structural Database (Figure 2). The data indicate that, for a *trans*-N–Co–O arrangement, there is a clear correlation of the Co–O and Co–N bond distances. A short Co–O distance gives rise to a relatively long *trans*-Co–N distance and vice versa. For the *cis*-N–Co–O arrangement, this effect is very small, if at all significant. Subsequently, the adjacent lengths of the C–N bonds are moderately related to the Co–O distances: Long Co–O bonds imply somewhat longer C–N distances. However, this effect is marginally significant. Consequently, a simple analysis of these geometrical parameters would suggest that the trans-effect is larger than the cis-effect. However, none of these effects could

(36) Jackman, L. M.; Sternhell, S. *Applications of NMR Spectroscopy in Organic Chemistry*, 2nd ed.; Pergamon Press: Oxford, 1969.

(37) Kostromina, N. A.; Reiter, L. G.; Golubkova, V. V. *Ukr. Khim. Zh.* **1980**, *46*, 1248.

(38) (a) Bramley, R.; Brorson, M.; Sargeson, A. M.; Schäffer, C. E. *Inorg. Chem.* **1987**, *26*, 314. (b) Mettendorf, R.; Buchem, R.; Tebbe, K.-F.; Wasgestian, F.; Lober, J. *Inorg. Chim. Acta* **1996**, *245*, 17. (c) Charland, J.-P.; Attia, W. A.; Randaccio, L.; Marzilli, L. G. *Organometallics* **1990**, *9*, 1367. (d) Toscano, P. J.; Brand, H.; Geremia, S.; Randaccio, L.; Zangrando, E. *Organometallics* **1991**, *10*, 713. Juranic, N.; Lichter, R. L. *J. Am. Chem. Soc.* **1983**, *105*, 406. (e) Juranic, N.; Macura, S. *Inorg. Chim. Acta* **1994**, *217*, 213. (f) Kofod, P.; Harris, P.; Larsen, S. *Inorg. Chem.* **1997**, *36*, 2258. (g) Storm, C. B.; Turner, A. H.; Rowan, N. S. *Inorg. Chem.* **1985**, *24*, 1269.

(39) Brodsky, N. R.; Nguyen, N. M.; Rowan, N. S.; Storm, C. B.; Butcher, R. J.; Sinn, E. *Inorg. Chem.* **1984**, *23*, 891.

(40) Orellana, G.; Ibarra, C. A.; Santoro, J. *Inorg. Chem.* **1988**, *27*, 1025.

Table 1. Optimized Bond Lengths (in angstroms)^a

distance	4 ³⁺	4-H ²⁺	6 ³⁺	6-H ²⁺	7 ³⁺	7-H ²⁺
Co–O	2.113	1.876	2.058	1.865	2.068	1.868
Co–N(trans)	1.955	2.000	1.979	2.051	2.005	2.074
Co–N(cis)	2.018, 2.022	2.001, 2.007	2.014–2.043	2.001–2.023	2.024–2.039	2.012–2.022

^a B3LYP/TZVP results.

directly account for the different shifting of the ^1H signals upon deprotonation. We have therefore applied quantum chemical calculations of the chemical shifts, using DFT methods that include explicitly spin–orbit effects.

4.3. Quantum Chemical Results and Discussion. Quantitative calculations of ^1H shifts by means of quantum chemistry tend to be generally somewhat more difficult than for other nuclei, due to the relatively small shielding range covered, and due to the sensitivity of the shifts to environmental and rovibrational effects.⁴¹ We will not account for solvation effects, as this would currently make the computations very difficult if not unfeasible. Solvent effects are expected to be generally large in the present systems, due to hydrogen bond interactions between the ligand amine and hydroxo/alkoxo functions of the positively metal complexes and water. However, there are indications that the observed qualitative trends in the ^1H deprotonation shifts are not affected by these interactions. In particular, we note that the observations of “normal” and “abnormal” deprotonation shifts are independently made for complexes of very different lipophilicity/hydrophilicity. For example, complex **4** (and partly complex **5**) exhibits a large lipophilic hydrocarbon surface, whereas complex **3** is expected to exhibit hydrophilic behavior, due to the positively charged ammonium groups on the surface. This insensitivity of the investigated ^1H shifts to solvation may be due to the fact that the specific solvation takes place at groups somewhat removed from the CH_2 groups of interest. We expect thus that our gas-phase calculations at a suitable quantum chemical level will reproduce at least the observed trends and should provide us with an explanation of their origin. Before comparing directly computed and experimental results for the aqua/hydroxo system **4**³⁺/**4**-H²⁺, we will in the following concentrate on simplified model complexes **6**³⁺ and **7**³⁺ that allow an easier analysis of the origin of the observed trends, due to the smaller size and lower computational effort required.

Full details of the optimized structures are provided in the Supporting Information (Table S2). Table 1 shows the metal–ligand distances for aqua and hydroxo forms of **4**, **6**, and **7**. Deprotonation of the aqua ligand generally shortens the Co–O bond appreciably, with a concomitant lengthening of the trans Co–N bond. Interestingly, the cis Co–N bonds shorten slightly upon deprotonation. These structural features will become important later in our discussions of deprotonation shifts.

Figure 3 shows the nonrelativistic chemical shifts calculated for the four protons H_A through H_D of the *en* ligand in **6**³⁺ and in **6**-H²⁺ (dashed lines, open symbols). These calculations would suggest a low-frequency shift upon deprotonation for all four hydrogen atoms. While this is consistent with the classical expectations discussed above, it provides no explanation for the experimental observation that protons of the CH_2 group attached to the amine nitrogen atom in the trans-position may exhibit a

high-frequency shift. We subsequently calculated spin–orbit (SO) corrections to the chemical shifts, using the triple-perturbation DFT approach of ref 30 (SO-corrected results as full lines with closed symbols). While the SO effects are negligible for positions H_B and H_D, a significant shielding is found for H_A and H_C. Notably, for H_C in the trans CH_2 group, the SO shielding is much more pronounced with the aqua complex than with the hydroxo complex, and it thereby inverts the overall deprotonation shift from a shielding (low-frequency) to a deshielding (high-frequency) one. This suggests that the observed high-frequency shift for certain CH_2 protons of the polyamine ligand upon deprotonation of the O(R)H ligand in the trans-position is due to a differential spin–orbit effect. It is notable that SO effects are also significant for H_A in the cis CH_2 group. However, here the shielding SO contributions are slightly larger for the hydroxo than for the aqua complex and thus add to a moderate “conventional” low-frequency shift upon deprotonation.

These findings give rise to further questions: (i) Which atom is responsible for the SO effects? (ii) Why is this SO effect, and thus the high-frequency deprotonation shift, operative only for certain protons of the polyamine ligand? (iii) Why is the shielding SO effect in the trans case larger in the aqua complex than in the hydroxo complex? To answer these questions, it is necessary to understand the nature of SO effects on nuclear shieldings. As has been discussed in detail recently,^{42,43} the third-order SO shifts are transmitted to the NMR nucleus mainly by a Fermi-contact-type mechanism (Figure 4). That is, the SO-induced spin polarization due to some heavy-atom center in the system has to be “felt” by the NMR nucleus in question via a Fermi-contact interaction with the surrounding spin density. A significant amount of spin density near this atom requires a spin-polarization pathway from the SO center, typically via the network of intervening bonds. As the Fermi-contact interaction operates via the spherical part of the spin density near the nucleus, in analogy to the Fermi-contact mechanism of indirect spin–spin coupling, significant s-character of the NMR atom for the bonds into this network is furthermore needed. The latter point is obviously fulfilled particularly well in the case of hydrogen atoms, which makes proton shifts the most sensitive to SO effects.^{42,43}

Question (i) may be answered easily by exploiting the effective atomic nature of the AMFI SO operators^{30–32} used in this work. This allows us to evaluate individually the SO effect coming from each atom in the system. As might be expected from the atomic numbers, our calculations show clearly that the SO effects on the ^1H shifts arise exclusively from SO coupling at the heaviest atom, the cobalt center (data not shown).

(42) Kaupp, M.; Malkina, O. L.; Malkin, V. G.; Pyykkö, P. *Chem.-Eur. J.* **1998**, *4*, 118.(43) Kaupp, M. Relativistic Effects on NMR Chemical Shifts. In *Relativistic Electronic Structure Theory II: Applications*; Schwerdtfeger, P., Ed.; Theoretical and Computational Chemistry Series; Elsevier: Amsterdam, 2004.(41) See, for example: Ruud, K.; Åstrand, P.-O.; Taylor, P. R. *J. Am. Chem. Soc.* **2001**, *123*, 4826.

Therefore, the observed SO effects are transmitted via three bonds, that is, along a Co–N–C–H pathway (Figure 4; see also below). We have previously demonstrated for the example of the β - ^1H -shift in iodoethane⁴² that the conformational dependence of such long-range SO shifts follows closely a Karplus-type behavior. This reflects again the close analogy between the Fermi-contact mechanisms of SO shifts (Figure 4) and that of indirect spin–spin coupling constants.^{42,43}

To evaluate whether the observation of large SO effects for H_C but not for H_D in the model complexes $6^{3+}/6\text{-H}^{2+}$ is related to such conformational dependencies, we calculated ^1H shifts and SO corrections to them for one CH_3 proton of a methylamine ligand in the simpler model complexes $7^{3+}/7\text{-H}^{2+}$ as a function of the H–C–N–Co dihedral angle (Figure 5). The nonrelativistic shifts of both complexes are moderately conformation dependent. However, as this dependence is similar for the aqua and hydroxo complexes, no large conformational dependence of the deprotonation shift is expected. The decisive observation is the appreciable conformational dependence of the SO shifts for the aqua complex (Figure 5) together with the much smaller SO effects for the hydroxo complex. In combination, this leads to a sizable conformational dependence of the deprotonation shifts. Notably, the SO shifts for the aqua complex reach their largest magnitude (ca. -1.2 ppm) close to a dihedral angle of 180° , that is, for an antiperiplanar arrangement (a second maximum of ca. -0.5 ppm is apparent for a synperiplanar arrangement). The SO effect for the hydroxo complex is also largest near $\pm 180^\circ$ but reaches only ca. -0.25 ppm. This translates into a deprotonation shift of about -1.0 ppm for an antiperiplanar arrangement, as compared to a negligible overall SO effect in the range of $\pm 80^\circ$. More generally, we see that the SO-corrected curve for the aqua complex is significantly below that for the hydroxo complex (indicating a high-frequency deprotonation shift) for absolute values of the dihedral angle above ca. 130° .

Examination of the dihedral angles in model complexes $6^{3+}/6\text{-H}^{2+}$ (cf. Figure 3 for atom labels) shows, indeed, that the dihedral angle for H_C is near 160° , that is, close to an antiperiplanar arrangement, whereas the dihedral angle for H_D is -80° . The conformational dependence of the SO shifts in model **7** thus provides readily an answer to part of question (ii): The protons of the CH_2 group in the trans-position of the aqua/hydroxo ligand will only show a significant “abnormal” SO-induced high-frequency shift upon deprotonation when their orientation is close to antiperiplanar with respect to the cobalt center. Notably, H_A of the cis CH_2 group in model **6** has an H–C–N–Co dihedral angle of 160° , again close to an antiperiplanar arrangement. Indeed, SO shifts in this case were notable (cf. Figure 3). However, in contrast to H_C , the SO effects are rather similar for the aqua and hydroxo complexes (actually somewhat larger for the latter, see Figure 3), and no anomalous deprotonation shift arises. H_B has a dihedral angle of -80° and correspondingly experiences small SO shifts in both complexes. We find thus that SO effects on the ^1H shifts are strongly conformation dependent for both cis and trans CH_2 groups, but only in the trans-position does this translate into an abnormal high-frequency shift upon deprotonation.

This brings us to question (iii), the origin of the much larger SO effects for the aqua than for the hydroxo complex in the case of H_C in model $6^{3+}/6\text{-H}^{2+}$ (Figure 3), and in the case of

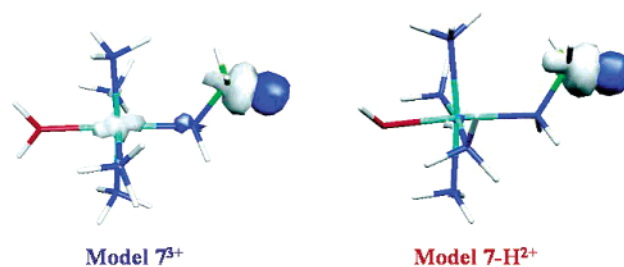


Figure 6. Spin-density distribution induced by a finite Fermi-contact perturbation ($\lambda = 0.001$ au) on the antiperiplanar hydrogen atom: (a) 7^{3+} ; (b) 7-H^{2+} .

model $7^{3+}/7\text{-H}^{2+}$ (Figure 5). As discussed above, the SO-induced spin polarization has to be transferred to the hydrogen nucleus via the three-bond Co–N–C–H pathway. As is obvious from Figure 2, and from the optimized bond lengths (see Table 1), the much better donor abilities of the hydroxo ligand as compared to those of the aqua ligand weaken and lengthen the Co–N bond in the trans-position significantly. This may be expected to deteriorate the spin-polarization transfer and to cause less pronounced SO effects in the hydroxo complex. To test this hypothesis, we have introduced a finite Fermi-contact perturbation to a hydrogen atom in model $7^{3+}/7\text{-H}^{2+}$ in antiperiplanar conformation and have monitored the induced spin density due to this perturbation (Figure 6). The comparison between the aqua and hydroxo complexes shows clear differences in the induced spin-density distributions: While significant spin density on the cobalt atom and some spin density on the coordinated nitrogen atom is apparent for the aqua complex, the spin density is largely localized to the perturbed hydrogen atom in the hydroxo complex. This confirms that the weakening of the Co–N bond by the trans-effect of the hydroxo ligand destroys partly the Fermi-contact pathway responsible for the SO shifts, whereas the Fermi-contact mechanism remains much more pronounced for the aqua complex. We may now also understand why the SO effects were significant for H_A in model **6** for both the aqua and the hydroxo complex, and why SO effects do therefore not induce anomalous pH dependencies for the ^1H shifts of the cis CH_2 groups. In this case, no appreciable weakening of the corresponding Co–N bonds occurs upon deprotonation (in fact, the cis Co–N bond lengths contract slightly upon deprotonation of the aqua ligand; see above). Differential SO effects between protonated and deprotonated complexes remain small and actually enhance slightly the “normal” low-frequency shift upon deprotonation. We note in passing that the calculations provide us not only with the isotropic shieldings but with the full shielding tensors and with their orientation. We will refrain from discussing the details of the tensors but should mention that the most shielded component of the nonrelativistic shielding tensor is oriented along the C–H bond axis, with two more deshielded components (which are not identical, due to the low local symmetry) perpendicular to it. In contrast, the shielding SO contributions arise almost exclusively from the perpendicular directions and thereby reduce the anisotropy of the overall shielding tensor. This is analogous to observations with SO effects due to halogen substituents.^{42,43} The fact that the SO effects point into the shielding direction is in turn related^{30b,43,44} to the π -character of the decisive occupied

(44) Kaupp, M.; Malkina, O. L.; Malkin, V. G. *J. Comput. Chem.* **1999**, *20*, 1304.

Table 2. Comparison of Computed and Experimental Shifts for **4**³⁺/**4**-H²⁺ ^a

	dihedral angle ^b	exp. 4 ³⁺	NR ^c 4 ³⁺	NR+SO ^d 4 ³⁺	exp. 4 -H ²⁺	NR ^c 4 -H ²⁺	NR+SO ^d 4 -H ²⁺	Δexp. (4 -H ²⁺ / 4 ³⁺)	ΔNR ^c (4 -H ²⁺ / 4 ³⁺)	ΔNR+SO ^d (4 -H ²⁺ / 4 ³⁺)
H _A	150	2.05	3.12	2.26	2.45	3.23	3.01	+0.40	+0.11	+0.75
H _B	-92	2.33	2.08	2.06	2.44	2.32	2.32	+0.10	+0.24	+0.26
H _C	139	2.78	3.52	3.08	2.76	3.14	2.88	-0.06	-0.38	0.20
H _D	130	2.74	3.42	3.09	2.67	2.89	2.70	-0.08	-0.53	-0.39
H _E	-112	2.63	2.98	2.89	2.52	2.73	2.66	-0.10	-0.25	-0.23
H _F	-104	2.45	2.53	2.47	2.40	2.53	2.51	-0.05	-0.02	+0.04

^a Assignment based on the closest match between computed and experimental pH-dependence. ^b Co–N–C–H dihedral angles in optimized structures. Atom labels are consistent with Figure 1d. ^c Nonrelativistic result. ^d Result after SO correction.

highest occupied molecular orbitals involved (deriving from t_{2g} symmetry for an ideal octahedron) relative to the Co–N and C–H bonds.

The theoretical analyses indicate the SO origin of the observed anomalies. Indeed, the conformational dependencies and the breakdown of the Fermi-contact spin-polarization pathway due to the trans-effect of the hydroxo ligand are nicely consistent with our existing understanding of SO effects on NMR chemical shifts.^{42,43} What is striking in the present case, however, is the surprising magnitude of the long-range SO effects given the relatively low atomic number of cobalt (27). The three-bond SO effects found here are of the same order as those identified previously for the β-hydrogen atom in iodoethane,⁴² where the SO effects are due to iodine SO coupling (atomic number 53)!

Equation 1 provides a third-order perturbation expression for the SO corrections to nuclear shieldings.^{43,45}

$$\sigma_{N,uv}^{\text{SO-I-K}} = \frac{\partial^2}{\partial \mu_{N,u} \partial B_{0,v}} \times \left[\sum_{m,n \neq 0} \frac{\langle 0 | \mathbf{H}^{\text{K}} | m_{\text{T}} \rangle \langle m_{\text{T}} | \mathbf{H}^{\text{SO(i)}} | n_{\text{S}} \rangle \langle n_{\text{S}} | \mathbf{H}^{\text{B}_0} | 0 \rangle}{(E_0 - {}^3E_m)(E_0 - {}^1E_n)} + \text{permutations} \right] \quad (1)$$

Here, μ denotes the nuclear magnetic moment, and \mathbf{B} is the external magnetic field. The total energies E in the denominator and the wave functions in the matrix elements in the numerator pertain to ground and triplet or singlet excited states of the system, and the double sum runs over all of the excited states. \mathbf{H}^{K} in the first matrix element denotes hyperfine operators, in the present discussion mainly the Fermi-contact operator. The second and third matrix elements account for SO operators and external magnetic field, respectively. The magnitude of the SO shielding contributions should depend linearly on the spin-orbit coupling of the relevant ground and excited states. It should therefore roughly increase with the square of the atomic number.⁴⁶ However, the energy denominator contains squares of energy differences. Closer inspection of the relevant MO contributions to the SO shifts in the present case shows that we may concentrate our discussion almost exclusively on the relevant ligand-field transitions of the cobalt d⁶ complex. The rather small ligand-field transition energies for a 3d metal, as compared to the much larger energies of the lowest-energy transition for a main-group molecule like iodoethane, provide an explanation why for the present systems the SO effects are appreciable even for a relatively light metal like cobalt.

(45) Vaara, J.; Ruud, K.; Vahtras, O. *J. Chem. Phys.* **1999**, *111*, 2900.

(46) See, for example: Pyykkö, P. *Chem. Rev.* **1988**, *88*, 563.

To be able to compare theory and experiment directly at least for one system, we have in addition to the smaller models also computed the ¹H shifts for the pair of complexes **4**³⁺/**4**-H²⁺, based on fully optimized structures. The results are shown in Table 2, both at the nonrelativistic level and with SO corrections added. As experimental values for comparison, we have used the values obtained from the (Σ(δ_{obs} - δ_{calc})² = min) fitting procedure (Table S1). Assignment to the different positions H_A–H_F is based (i) on the best fit of deprotonation shifts, (ii) on the additional information known from experiment (see section 4.1), and (iii) for H_C–H_F also on the best agreement with individual shifts. As discussed in the Details of Quantum Chemical Calculations section, we cannot expect complete quantitative agreement for various reasons. When the deprotonation shifts Δδ are compared, our SO-corrected results (ΔNR+SO) tend to overshoot as compared to the experiment results (Δexp), both in the positive and in the negative directions. Notably, however, the trends are reproduced correctly, except for the sign of the particularly small deprotonation shift of H_F. In particular, we identify the large positive deprotonation shift for H_A with a hydrogen atom of a trans CH₂ group with a dihedral angle close to antiperiplanar. As expected from the discussion above, the abnormal deprotonation shift is dominated clearly by differential SO effects (although a small deshielding is already computed at the NR level). Interestingly, however, position H_B, which has a dihedral angle near 90° and thus almost negligible SO effects, exhibits a small positive deprotonation shift already at the NR level. This contrasts to the smaller models **6** and **7**, where the nonrelativistic calculations always produced a negative deprotonation shift. This suggests that, while the SO effects are clearly responsible for most of the “abnormal” shift behavior, small effects may arise already at the nonrelativistic level. This has to be viewed with some caution, however, given the smallness of these additional effects and the inherent error bars of the calculations.

Moving on to the protons in the cis-position, we find significant individual SO effects on the shifts of H_C and H_D and much smaller ones for H_E and H_F. This is consistent with the much larger dihedral angles for the former pair of hydrogen positions (see discussion of conformational dependence above). Notably, in all four cases, the SO shifts are slightly larger for the aqua complex **4**³⁺ than for the hydroxo complex **4**-H²⁺. This contrasts to our above results for H_C in model **6**³⁺/**6**-H²⁺ and leads to a slight reduction of the negative deprotonation shifts for H_C–H_E (and to a sign change for H_F). In any case, the results for the realistic complex **4** confirm largely the conclusions drawn from the smaller models **6** and **7**: (a) Shielding SO effects are pronounced only for approximately antiperiplanar H–C–N–Co arrangements, whereas they remain very small for perpen-

dicular or gauge conformations. (b) In the trans-position, the SO shifts are much larger for the aqua than for the hydroxo complex and thereby cause abnormal high-frequency deprotonation shifts. (c) In the cis-position, the differences between the SO effects for aqua and hydroxo complexes are much smaller, and thus no abnormal shifts are found.

5. Conclusions

In this paper, we have described a specific cis- and trans-effect for the ^1H NMR signal of a $\text{H}-\text{C}-\text{N}(\text{R}_2)-\text{Co}-\text{O}(\text{R})-\text{H}$ substructure. Deprotonation of the oxygen donor resulted in a characteristic shift to higher frequency for the trans-geometry and to lower frequency for the cis-geometry. The different behavior can readily be seen in an NMR titration experiment, and this represents an efficient tool for the structure elucidation of such molecules. As an example, we have demonstrated that the different acidic sites in a polyaqua or polyalcohol complex such as $[\text{Co}(\text{tren})(\text{H}_2\text{O})_2]^{3+}$ or $[\text{Co}(\text{tach})(\text{ino}-\kappa^2-\text{O}^{2,4}-\kappa-\text{N}^3)]^{3+}$ can be readily identified by this method. Moreover, the approach could also prove useful for the identification of the different $\text{Co}-\text{N}-\text{C}-\text{H}$ fragments in a species having a polyamine portion as part of a more complex structure. As an example, $[\text{CoL}(\text{H}_2\text{O})_2]^{3+}$ complexes with a flexible linear tetraamine ligand L can exist as cis or trans isomers. The identification of the different isomers could readily be achieved by taking advantage of this effect. We have further demonstrated that the anomalous pH-dependence of certain ^1H chemical shifts is generally observable for primary, secondary, and tertiary amines as well as for water and polyalcohols as oxygen donors. The computationally determined conformational dependence of the effect is potentially important for conformational analyses of the coordinated ligands.

From a theoretical point of view, it is of particular interest that the “abnormal” pH-dependence of some of the CH_2 protons in the trans-position of the polyamine ligands is due to a long-range (three-bond) spin-orbit contribution to the chemical shift, originating from spin-orbit coupling at the d^6 cobalt(III) metal center. Due to the pronounced trans-effect of anionic ligands, the Fermi-contact mechanism that transmits these spin-orbit effects to the hydrogen nuclei is much more efficient for the aqua (alcohol) complex than for the hydroxo (alkoxo) deprotonation product. The resulting differential spin-orbit effect leads largely to the observed characteristic high-frequency deprotonation shifts. The observations may be explained readily

using a recently developed analogy between spin-orbit chemical shifts and the Fermi-contact mechanism of indirect spin-spin coupling.^{42,43} In particular, the conformational dependencies are due to a Karplus-type relation of the spin-polarization transfer to the dihedral angle. The lower spin-orbit shifts for the deprotonated species may be rationalized by an interruption of the transfer pathway.

While the results of the theoretical analysis are thus consistent with our current understanding of spin-orbit effects on chemical shifts,^{42,43} the appreciable magnitude of the observed long-range effects in the present cobalt complexes came as a surprise, given the relatively small spin-orbit coupling constant of the 3d metal cobalt. We attribute this to the small excitation energies entering the perturbation expression for the spin-orbit shifts, due to the small ligand-field splitting in the 3d series. Preliminary computational results on analogous rhodium and iridium complexes⁴⁷ suggest that the spin-orbit shifts grow much less down the group than expected from the usual Z^2 dependence⁴⁶ of spin-orbit coupling. This is due to the opposing effect of a growing ligand-field splitting for the heavier metals. We may expect analogous long-range spin-orbit effects on chemical shifts also for other diamagnetic transition metal complexes.

Acknowledgment. Work in Saarbrücken and in Würzburg has been supported by the Fonds der Chemischen Industrie. Work in the Würzburg group has in particular been funded within the Deutsche Forschungsgemeinschaft DFG project KA1187/5-1, and by a postdoctoral scholarship to M.S. within the graduate college “Moderne Methoden der magnetischen Resonanz in der Materialforschung” at Universität Stuttgart. We thank Dr. Bernd Morgenstern, Michael Mentges, and Barbara Kutzky for performing a series of NMR titration experiments. Technical assistance by Dr. Roman Reviakine in Würzburg with the quantum chemical computer codes is gratefully acknowledged.

Supporting Information Available: One table (S1) with NMR titration results and one table (S2) with Cartesian coordinates of computationally optimized structures. This material is available free of charge via the Internet at <http://pubs.acs.org>.

JA0316723

(47) Straka, M.; Reviakine, R.; Kaupp, M., unpublished results.